Mol. Hum. Reprod. Advance Access published January 31, 2006
doi:10.1093/molehr/gal007

Crossover frequency and synaptonemal complex length: their variability and effects on human male meiosis

M.Codina-Pascual[1,5], M.Campillo[2], J.Kraus[3,4], M.R.Speicher[3,4], J.Egozcue[1], J.Navarro[1] and J.Benet[1,5]

[1]Unitat de Biologia Cel.lular i Genètica Mèdica, Departament de Biologia Cel.lular, Fisiologia i Immunologia, [2]Laboratori de Medicina Computacional, Unitat de Bioestadística, Universitat Autònoma de Barcelona, Bellaterra, Spain, [3]Institut für Humangenetik, Technische Universität, München and [4]GSF – Gesellschaft für Umwelt und Gesundheit, Neuherberg, Germany

[5]To whom correspondence should be addressed at: Departament de Biologia Cel.lular, Fisiologia i Immunologia, Universitat Autònoma de Barcelona, Bellaterra 08193, Spain. E-mail: jordi.benet@uab.es\montserrat.codina@uab.es

In this study, immunocytogenetics has been used in combination with the subtelomere-specific multiplex-fluorescent in-situ hybridization (stM-FISH) assay to identify 4681 autosomal synaptonemal complexes (SCs) of two fertile men. Comparisons of crossover maps for each individual SC between two men with extremely different meiotic crossover frequencies show that a low crossover frequency results in (i) a higher frequency of XY pairs and of small SCs without MLH1 foci and (ii) lower frequency of crossovers in the proximity of centromeres. In both cases, the bivalents which most frequently lacked MLH1 foci were the XY pair and the SC21. Analysis of SC length showed that SC arms can be longer or shorter than the corresponding mitotic one. Moreover, for a given SC, the variation in length found in one arm was independent of the variation observed in the other one (e.g. SC1p arms are longer than SC1q arms). The results confirmed that reduction in the crossover frequency may increase the risk of achiasmate small bivalents and that interindividual differences in crossover frequency could explain the variability in the frequencies of aneuploidy in human sperm. How MLH1 foci are positioned within the SC is discussed based on detailed MLH1 foci distributions and interfoci distances. Finally, evidence that the variation of the SC arm length may reflect the abundance of open and of compact chromatin fibers in the arm is shown.

Key words: aneuploidy/human crossover maps/meiosis/stM-FISH/synaptonemal complex

Introduction

Meiotic recombination contributes to genetic variability and to the proper completion of the meiotic process. In mammals, meiotic recombination starts early in meiotic prophase I before the synapsis of homologous chromosomes. In mammals, as in yeast, meiotic recombination is initiated by Spo11-dependent DNA double-strand breaks (DSB) at leptotene stage (Baudat *et al*., 2000; Romanienko and Camerini-Otero, 2000; Mahadevaiah *et al*., 2001). DSBs activate the DNA repair process in which several proteins are involved (reviewed in Svetlanov and Cohen, 2004). During the DNA repair process only a few of these DSBs will be designated as crossovers by the onset of single-end invasions (SEIs) formation (Hunter and Kleckner, 2001; Börner *et al*., 2004). Afterwards, double Holliday junctions (dHjs) are formed, resolved and cytologically seen as late recombination nodules. Several homologues of yeast proteins involved in the initiation, consolidation and resolution of the recombination events have been described in mammals and humans (reviewed in Svetlanov and Cohen, 2004) (Roig *et al*., 2004; Oliver-Bonet *et al*., 2005). Some of these proteins specially localize to recombination foci that will result in crossovers (e.g. MLH1; Baker *et al*., 1996; Barlow and Hultén, 1998).

Direct and indirect methods have been used for the study of human male meiotic recombination. Analyses of genotype data in CEPH and deCODE families have indirectly allowed the generation of human male and female genetic maps (Broman and Weber, 2000; Kong *et al*., 2002; Matise *et al*., 2003). These linkage maps can be used to deduce the location of crossover events. For years, the observation of chiasmata in meiotic chromosomes has been the only direct method of analysis of crossovers. This method resulted in the first physical description of frequency and distribution of crossovers in human males (Hultén, 1974; Laurie and Hultén, 1985a,b). Of late, the characterization of proteins that recognize the sites of crossing over (e.g. MLH1) and of proteins present in the synaptonemal complex (SC) (e.g. SCP1 and SCP3) has allowed for the study of meiotic recombination between homologous chromosomes using direct immunocytogenetic detection. This new methodology has enabled the first visualization of human male and female recombination foci at pachytene on SC spreads (Barlow and Hultén, 1998; Tease *et al*., 2002). Several studies have applied the immunocytogenetic method for meiotic analysis in human males and described a high interindividual variation in crossover frequencies (Hassold *et al*., 2004; Codina-Pascual *et al*., 2005; Sun *et al*., 2005). This variation in the frequency of crossing over could be the reason for the high variability in the frequency of aneuploidy in human sperm (reviewed in Hassold and Hunt, 2001; Templado *et al*., 2005). Moreover, this immunocytogenetic labelling can be followed by fluorescent in-situ hybridization (FISH) methods for SC identification. Recently, the development of several multiplex-FISH strategies has allowed the simultaneous identification of every SC in a given spermatocyte (Oliver-Bonet *et al*., 2003; Codina-Pascual *et al*., 2004). The successive application of immunocytogenetics and multiplex-FISH has been used to describe the distribution of meiotic recombination events for each SC in a human male (Sun *et al*., 2004).

In the present work, the distribution of meiotic crossover events in two selected men has been analyzed and compared by combining immunocytogenetics (SCP1, SCP3, MLH1 and CREST) and seven-fluorochrome subtelomere-specific multiplex-FISH (stM-FISH) methodologies. These two fertile men with high and low frequencies of crossing over, respectively, were studied to evaluate which SCs are more sensitive to the interindividual variability in crossover frequencies.

Materials and methods

Individuals included in the study were two men (C6, C7) of proven fertility. Testicular biopsies were obtained while undergoing vasectomy (C6) or vasectomy reversal (C7) under local anesthesia. Written consent was given by patients, and the study was approved by our Institutional Ethics Committee.

Sample treatment

Testicular tissue was processed for the immunocytogenetic analysis of SCs using a slight modification of the protocol previously described (Codina-Pascual *et al*., 2004). A piece of the biopsy was shredded in a 20 µl drop of 0.1 M sucrose. The drop containing free pachytene cells was spread on a slide covered with 1% paraformaldehyde/Triton-X solution, pH = 9.2. Slides were stored overnight at room temperature in a humid chamber. Afterwards, slides were allowed to dry and were then washed in 0.04% Photo-Flo (Kodak, Germany) for 4–10 min. Finally, after a short rinse in distilled water, they were air dried. The presence of cells was confirmed by microscopic evaluation. Slides were blocked with 0.05% milk powder solution in 4× SSC-0.05% Tween-20 (4× SSCT) for 30 min. Four primary antibodies were used: rabbit anti-SCP3 (Lammers *et al*., 1994) and rabbit anti-SCP1 (Meuwissen *et al*., 1992) (both gifts from Dr Christa Heyting), anti-CENP (CREST serum kindly provided by Dr William Earnshaw) and mouse anti-MLH1 (Pharmingen; San Diego, CA, USA). They were applied at 1:1000, 1:1000, 1:1000 and 1:250, respectively, in the blocking solution mentioned above, overnight, at 37°C. The combination of antibodies against SCP1 and SCP3, proteins of the central and lateral elements, respectively, ensures a high intensity signal for the SC labelling. Slides were washed in (1×) PBS for 48 h at 4°C. Afterwards, the secondary antibodies, tetramethylrhodamine B isothiocyanate (TRITC)-conjugated goat anti-rabbit immunoglobulin G (IgG) antibody and fluorescein isothiocyanate (FITC)-conjugated goat anti-mouse IgG antibody (both from Sigma, Madrid, Spain), were diluted in 1:250 blocking solution and applied for 3 h at 37°C. In a third round, the Pacific Blue-conjugated rabbit anti-human IgG (from Sigma) labelled with Zenon Reaction (Molecular Probes, Barcelona, Spain) was applied at 1:250 for 1 h. Finally, slides were washed, briefly rinsed in distilled water, air dried and counterstained with antifade (Vector lab Inc., Burlingame, CA, USA). An epifluorescence microscope (Olympus Bx60) and Power Macintosh G3 with Smartcapture software (Digital Scientific, Cambridge, UK) were used for cell evaluation and image capturing.

StM-FISH

DNA probes for the stM-FISH assay (Fauth *et al*., 2001) were prepared and applied as previously described (Codina-Pascual *et al*., 2004). Microdissected subtelomeric probes, with sizes between 5 and 10 Mb, were amplified and labelled by DOP (Degenerate oligonucleotide primer)–PCR according to a combinatorial labelling scheme based on seven different fluorochromes (Fauth *et al*., 2001). For direct labelling, DEAC (Perkin Elmer, Jügensheim, Germany), Cy3 and Cy5 (both from Amersham Pharmacia Biotech, Munich, Germany), TexasRed (Molecular Probes), dUTP-conjugates were used. DNP (Perkin Elmer), biotin and digoxigenin (both Roche Diagnostics, Mannheim, Germany), dUTP-conjugates were used for indirect labelling. After 48 h hybridization and post-hybridization washes, anti-DNP-KLH-Alexa488 (1:400; Molecular Probes), avidin-Cy5.5 (1:200; Rockland Inc., Gilbertsville, USA) and anti-digoxigenin-Cy7 (1:50; Cy7 from Amersham Pharmacia Biotech) were used for detection of hapten-labelled probes. Finally, slides were counterstained with DAPI and mounted in *p*-phenylenediamine dihydrochloride antifade solution (Merck, Darmstadt, Germany). Visualization was performed using a motorized epifluorescence microscope with an eight-position filter wheel (Leica DMRXA-RF8), a Sensys CCD camera (Photometrics; Kodak KAF 1400 chip) and the Leica QFISH software (Leica Microsystems Imaging Solutions, Cambridge, UK).

Cell analysis

Immunolabelled pachytene cells were captured. The identification of all SCs was performed by projection of the stM-FISH hybridization results into the image of the immunolabelled pachytene cell. Measurements of SC lengths and determination of centromere and recombination foci positions were made using the version 3.3 MicroMeasure program (available at http://www.colostate.edu/depts/biology/micromeasure). The number of MLH1 foci per autosomal SC and the presence of an MLH1 focus in the XY pair were evaluated.

Statistics

Statistical analysis was performed using the SPSS 13.0 program (SPSS Inc., Chicago, IL, USA). The χ^2 test and Fisher exact test, when necessary, were applied to percentage comparisons. The Student's *t*-test was applied to mean comparisons between both cases. Pearson's correlation coefficient was calculated to evaluate the strength of the relationship.

Results and discussion

A total of 213 pachytene cells from two fertile men were immunolabelled and consecutively hybridized with the subtelomere multiplex-FISH assay (stM-FISH) for SC identification. The subtelomere probe set labelled in a combinational way with seven different fluorochromes allowed for a high level of confidence and efficiency in autosomal SC identification (4681/4686, 99.9%), even in cases of overlapping SCs (Codina-Pascual *et al*., 2004) (Figure 1). Table I summarizes the number of cells analyzed and the MLH1 values for the two cases studied.

SC lengths

The length of each identified SC was measured, including heterochromatic blocks, and expressed as a mean of absolute (µm) and relative (%) lengths (Table II). The case showing the longest SCs (C7) was the individual with the highest meiotic recombination frequency (Table I). This is in agreement with the covariation described between SC length and number of crossover events (Lynn *et al*., 2002). Relative SC lengths showed no differences between the two individuals, therefore the analysis was done using the mean from C6 and C7. Relative SC lengths correlated with relative lengths of mitotic chromosomes (ISCN, 1985) ($P < 0.0001$, $r^2 = 0.96$). However, the relative length of some SCs was statistically longer (e.g. SC19, SC17, SC16 and SC15; $P < 0.001$) or shorter (e.g. SC4, SC8, SC13, SC14, SC18 and SC21; $P < 0.001$) than the relative length of the corresponding mitotic chromosome (Table II and Figure 2a).

When the p and q arms were analyzed separately, they usually showed variation of their relative length. For a given SC, the variation in length found in one arm was independent of the variation found in the other one (Figure 2b and c). This resulted in some SCs with centromere index different from the corresponding mitotic one (Table II). A clear example of this was SC1. Because stM-FISH only hybridizes to the subtelomeric region of the chromosome 1 q arm (Fauth *et al*., 2001; Codina-Pascual *et al*., 2004), SC1p and SC1q arms were unequivocally distinguished by the hybridization result. The measurement of the SC1 length (µm) showed that the SC1p arm was longer than the SC1q ($P < 0.0001$). The SC1p increased (13%) and the SC1q reduced (11%) their relative length in comparison with their mitotic counterparts (Figure 2b and c), and resulted in a centromere index of 0.54 for the SC1, versus 0.48 for the mitotic chromosome 1 (ISCN, 1985) (Table II). Nevertheless, the relative length of the whole SC1 did not differ from the mitotic one.

The human genome sequence shows that chromosomes have differences in the percentage of GC (Guanine and citosine) content and in gene density (Venter *et al*., 2001). R-bands are regions with a high GC content and gene density, whereas G-bands are poor in GC and in genes.

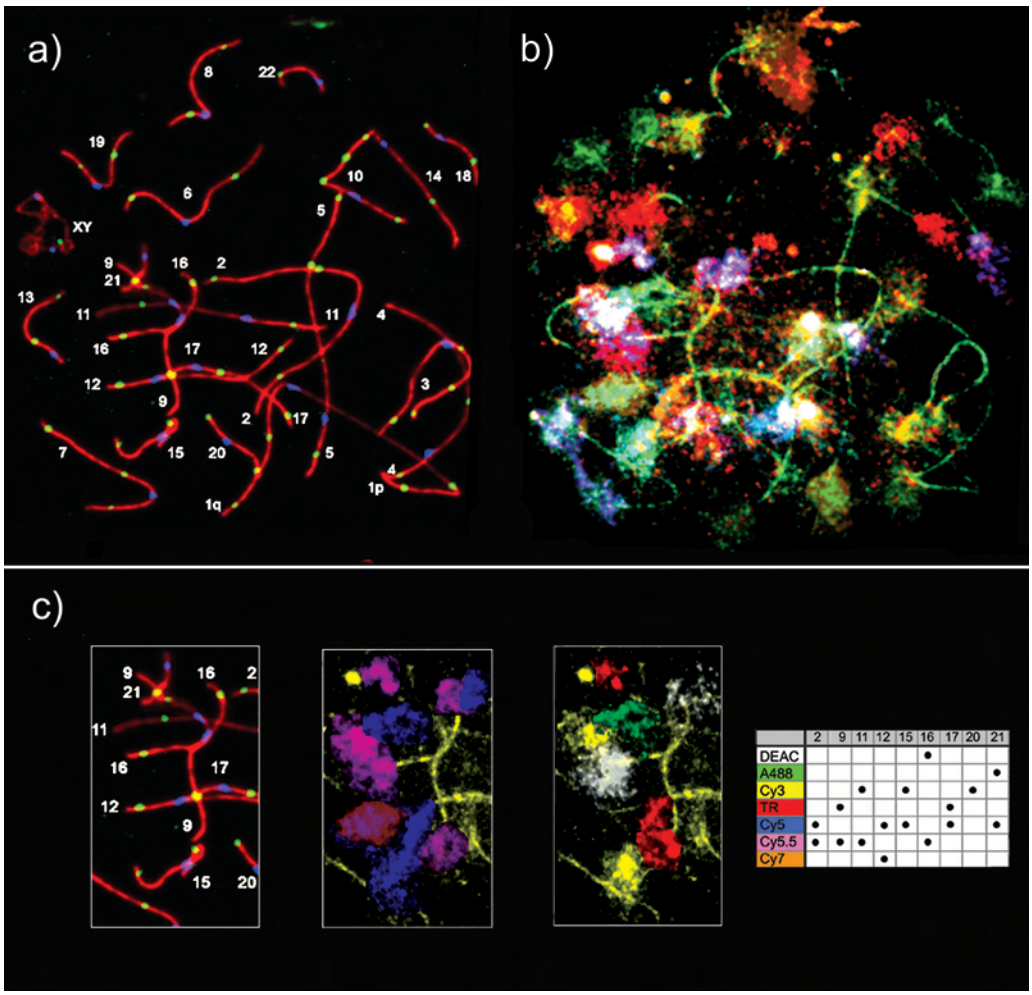

Figure 1. (**a**) Human pachytene spermatocyte with all synaptonemal complexes (SCs) identified. SCs are immunolabelled in red (SCP1 and SCP3), centromeres in blue and MLH1 foci in yellow. (**b**) Corresponding composite subtelomere-specific multiplex-fluorescent in-situ hybridization (stM-FISH) image. (**c**) Example of identification of overlapped SCs. Detail of the overlapped SC (upper left). DEAC, Alexa488, Cy3 and TexasRed channels (lower right) are shown separately from Cy5, Cy5.5 and Cy7 (upper right). Colour combination for each SC is shown in the scheme table (lower left).

Table I. MLH1 foci number and autosomal synaptonemal complex (SC) length in pachytene spermatocytes

Case	Cells (*N*)	MLH1 in autosomes			MLH1 per cell			MLH1 in XY (% cells)
		Mean	SD	MLH 1/10 µm	Mean	SD	Range	
C6	105	42	3.8	1.53	42.6	3.9	32–52	62.9
C7	108	52.2	5.6	1.54	53	5.7	35–63	74.1
Total/mean	213	47.1	1.53	47.8	32–63	68.5		

Among R-bands, T-bands have the highest gene density, the longest genetic distance (Holmquist, 1992) and are regions of abundant open chromatin fibers (Gilbert *et al*., 2004). It is herein shown that those SCs with a relative length longer than the mitotic relative length are those having regions with high GC content and gene density (R-bands). Conversely, those SCs with a shorter relative length have abundant regions with low GC content and gene density (G-bands). Similar to the whole SC, the SC arms that showed a higher increase of their relative lengths are rich in GC content and in gene density (Figure 2b, c, e and g; SC1p arm, both arms of SC19 and SC17, and the SC22q arm). In general, the variation in the SC relative length, expressed as the percentage of difference between SC and mitotic chromosome relative lengths, positively correlated with the gene density of the chromosome ($P < 0.0001$, $r^2 = 0.8$) (Figure 3). It is interesting to note that the scatterplot graph shown in Figure 3 has a great similarity to that published by Gilbert *et al*. (2004), in which a correlation between the abundance of open chromatin fibers and gene density is shown. It has been reported that heterochromatin represents a shorter region in the pachytene chromosome than in the mitotic chromosome and that SC in heterochromatic regions is under-represented and densely sheathed in highly compact chromatin (Stack, 1984). Taking all these data together, it is possible that the variation in the SC relative length may reflect the amount of open and compact chromatin fibers present in the chromosome. Regions of open chromatin fibers are cytologically decondensed in human lymphoblasts (Gilbert *et al*., 2004). Therefore, the chromatin present in R-bands and in T-bands is in a more decondensed state and has a larger volume than the chromatin in G-bands (Yokota *et al*., 1997; Gilbert *et al*., 2004). Conversely, heterochromatin is in a more condensed state and has a smaller volume in pachytene nuclei (Stack, 1984). According to the dual-loop module model, which proposes that the number of loops positively correlates with the AE (Axial element) length (Kleckner *et al*., 2003), chromosome regions with open chromatin fibers may present more chromatin

Table II. Lengths for each autosomal synaptonemal complex (SC)

SC	Absolute SC length (μm)				Relative SC length (%)		SC centromere index		Mitotic chromosome	
	C6		C7		Cases mean	SD	Cases mean	SD	Relative length	Centromere index
	Mean	SD	Mean	SD						
1	23.76	3.35	29.61	4.20	9.12	0.56	0.54*	0.02	9.11	0.48
2	21.52	3.15	27.23	4.27	8.31	0.60	0.39	0.03	8.61	0.39
3	17.69	2.78	21.88	3.32	6.75	0.55	0.47	0.02	6.97	0.47
4	14.48	2.25	19.28	3.58	5.73*	0.56	0.28	0.03	6.49	0.28
5	15.42	2.31	19.90	3.46	6.01	0.53	0.25**	0.02	6.21	0.27
6	14.38	1.92	18.83	3.59	5.65**	0.50	0.41*	0.03	6.07	0.38
7	15.19	2.41	18.62	2.82	5.77**	0.51	0.36	0.03	5.43	0.37
8	11.68	1.58	14.77	2.23	4.51*	0.35	0.33	0.02	4.94	0.33
9	12.55	1.64	15.79	2.91	4.83	0.46	0.31	0.03	4.78	0.33
10	12.12	1.66	14.79	2.33	4.60	0.33	0.30*	0.02	4.8	0.32
11	12.62	2.04	15.23	2.38	4.76	0.42	0.38**	0.02	4.82	0.41
12	12.67	1.81	15.65	2.88	4.83**	0.40	0.26	0.02	4.5	0.27
13	8.30	1.03	10.33	1.40	3.18*	0.21	0.08*	0.02	3.87	0.17
14	8.91	1.21	10.85	1.61	3.38*	0.25	0.08*	0.02	3.74	0.18
15	9.89	1.38	11.70	1.77	3.70*	0.30	0.09*	0.02	3.3	0.18
16	9.60	1.20	11.06	1.69	3.54*	0.27	0.45**	0.02	3.14	0.43
17	10.20	1.13	11.77	1.61	3.78*	0.31	0.33	0.03	2.97	0.32
18	6.41	0.74	7.80	0.97	2.43*	0.15	0.28	0.02	2.78	0.27
19	9.21	1.04	10.42	1.41	3.38*	0.30	0.44	0.02	2.46	0.45
20	6.45	0.70	7.43	0.86	2.38**	0.18	0.40*	0.03	2.25	0.46
21	3.57	0.40	4.66	0.58	1.41*	0.14	0.18*	0.05	1.7	0.29
22	5.26	0.59	5.96	0.73	1.93**	0.17	0.11*	0.02	1.8	0.28
Total	261.9		323.6							

Relative SC length = (SC length/total length of SC set) x 100. Relative SC lengths and centromere indexes were compared to the mitotic values in the ISCN (1985).
*$P < 0.001$.
**$P < 0.05$.

attachment sites to the AE core resulting in longer SCs regions. Conversely, chromosome regions of compact chromatin may present fewer chromatin attachment sites and shorter SC regions. Recently, it has been suggested that a relationship between SCP3, by compacting the chromosome axis, and SMC1b, by defining chromatin loop attachment sites, is essential to establish a proper AE length (reviewed in Revenkova and Jessberger, 2005). The fact that the distribution of open and compact chromatin fibers is not uniform along the entire chromosome may explain the independent variation of relative length observed between SC arms.

MLH1 count

The mean number of MLH1 foci observed per autosomal SC set was 42 ± 3.8 for C6 and 52.2 ± 5.6 for C7. The two values are significantly different between them ($P < 0.0001$) and close to the lowest and the highest values in the recombination range described for human males, respectively (Table I). If these two fertile cases are included in our control series previously reported (Codina-Pascual *et al*., 2005), the mean frequency of recombination foci per autosomal SC in our control series is 47.8 ± 3.5. This value increases to 48.5 ± 3.6 if the MLH1 focus in the XY pair is included. Considering that each MLH1 occurs in a 50 cM interval (50% probability of a recombinant product), the mean genetic lengths are 2100 cM and 2610 cM for C6 and C7, respectively. Despite the differences in the frequency of MLH1 foci between both individuals, their recombination focus density was very similar: 1.5 MLH1/10 μm (Table I). This similar density is explained by the differences between absolute SC lengths of both cases, which covaries with the crossover frequency (Lynn *et al*., 2002).

MLH1 foci for each identified autosomal SC were also scored. Table III summarizes the average number of MLH1 foci in each SC obtained from the two cases. In general, autosomal SCs had at least one MLH1 focus. However, a few SCs displayed no MLH1 foci (Table IV), and, among these, SC21 was by far the one that most frequently lacked it. The incidence of SC21 without MLH1 focus was similar in both donors. But, in general, the incidence of SCs without MLH1 focus was higher for the C6 case ($P<0.05$).

Evaluation of the localization of MLH1 foci within the 44 autosomal p and q arms was carried out. The presence of an MLH1 focus in the p arm of acrocentric bivalents was seldom seen, only in the case of high crossover frequency (C7): 3% for the large acrocentric chromosomes (D group) and 2.3% for the small acrocentric chromosomes (G group). The absence of an MLH1 focus in one of the SC arms was more frequently observed in the small non-acrocentric SCs (i.e. SC17, SC18, SC19, SC20) ($P < 0.05$) and generally affected the p arm. The C6 individual, with a low crossover frequency, showed a higher incidence of these SCs with no MLH1 focus in one of their arms than the C7 ($P < 0.0001$ for SC18 and SC20; $P < 0.05$ for SC17 and SC19).

The presence of an MLH1 focus in the XY pair was also analyzed and was observed in 62.9 and in 74.1% of the XY pairs for C6 and C7, respectively (Table I). The lowest value corresponds to the case with the lowest MLH1 foci count in autosomal SCs. This result corroborates our previous observation of a correlation between the frequency of cells with an MLH1 focus in the XY pair and the total number of autosomal crossover foci per cell (Codina-Pascual *et al*., 2005).

It is known that at least one crossover event must occur in each SC to ensure its proper meiotic segregation and that reduced crossing over frequency may increase the risk of univalents at metaphase I (reviewed in Egozcue *et al*., 2000) and of chromosome aneuploidy (reviewed in Hassold and Hunt, 2001). According to the results, the XY pair and bivalent 21 would be the most prone to become achiasmate,

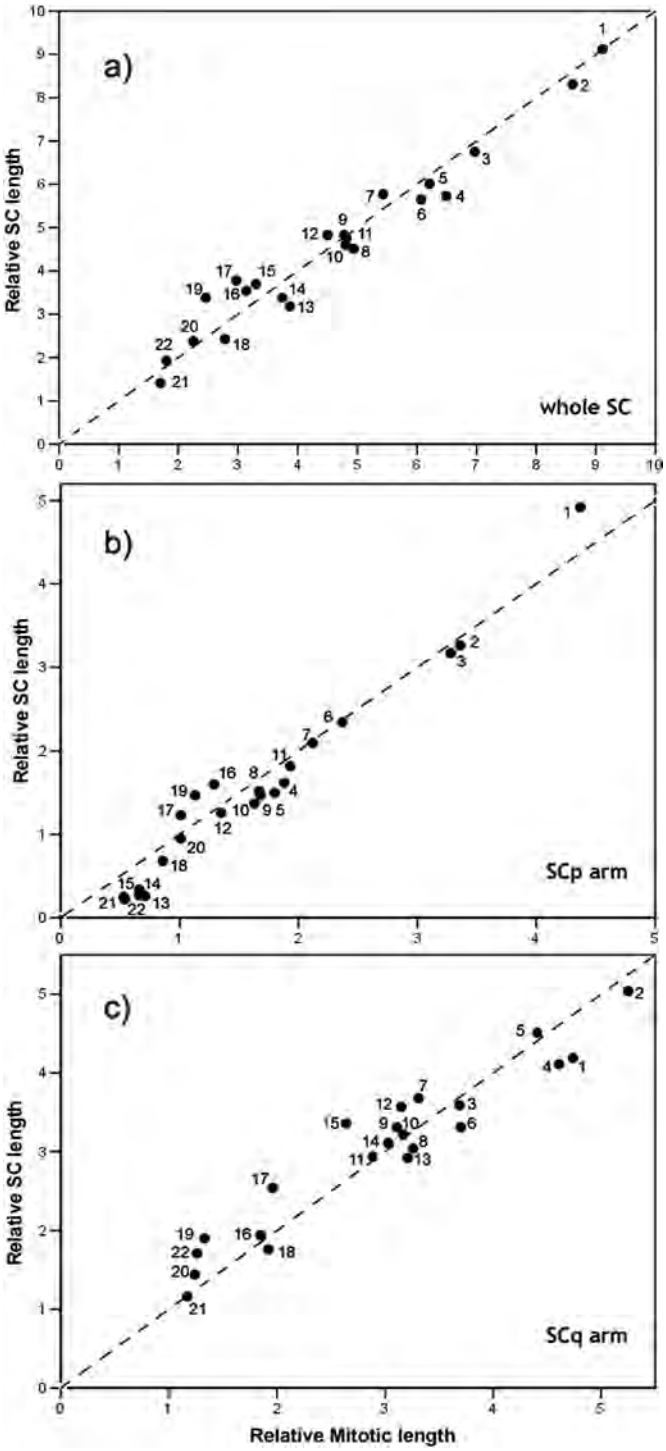

Figure 2. Synaptonemal complex (SC) and mitotic relative length (ISCN, 1985) scatterplots for individual SCs when the whole SC (**a**), SCp arm (**b**) and SCq arm (**c**) are considered ($P < 0.0001$; $r^2 = 0.96$, $r^2 = 0.96$ and $r^2 = 0.92$, respectively). The diagonal lines ($r^2 = 1$) correspond to a 1:1 relation between SC and mitotic relative lengths. Values over this line indicate SC > mitotic; values close to the line indicate SC ~ mitotic; values under the line indicate SC < mitotic.

followed by bivalents 22, 19 and 18, in decreasing order (Table IV). This observation is consistent with the most frequently observed chromosome aneuploidies in sperm nuclei of normal men, i.e. disomies of sex chromosomes and of chromosomes 21 and 22 (reviewed in Templado *et al*., 2005). Chromosomes 19 and 18 have been described to be

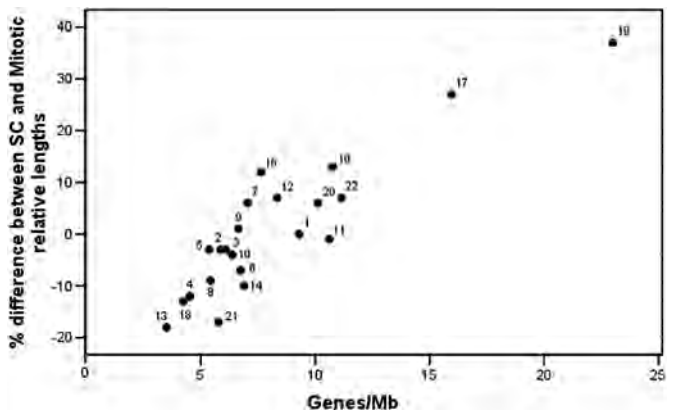

Figure 3. Scatterplot between the variation of synaptonemal complex (SC) relative length and gene density for individual SCs (Ensembl genes/Mb). The variation of the SC length is expressed as the percentage of difference between SC and mitotic relative lengths [% difference = [(relative SC length/relative mitotic chromosome length)-1] x (100)] ($P < 0.0001$; $r^2 = 0.8$).

involved in univalency in a study in which multiplex-FISH was applied on male meiotic divisions (Sarrate *et al*., 2004). Increased chromosome 19 aneuploidy has also been described in female meiosis (Clyde *et al*., 2003; Gutiérrez-Mateo *et al*., 2004). This is consistent with studies in which reduced recombination is found in disomic 24,XY sperm heads (Shi *et al*., 2001) and in cases of paternally derived trisomy 21 (Savage *et al*., 1998) and 47,XXY (Hassold *et al*., 1991; Thomas *et al*., 2000). However, it is worth noting that the frequencies of aneuploidy in human sperm observed for sex chromosomes and chromosomes 21, 22, 19 and 18 are lower than the frequencies of these SCs with no MLH1 focus. Bivalents without a crossover event may induce a meiotic arrest before first meiotic division and do not proceed as univalents. However, a reduced number of them may avoid the meiotic checkpoints and result in aneuploidy.

Finally, the fact that the C6 case, with a low crossover frequency, displays a higher incidence of small SCs without an MLH1 focus in one or both arms than the C7 suggests that the C6 may have a higher risk of missegregation of small bivalents than the C7. However, this should be confirmed by meiotic analysis in metaphase I spermatocytes or in sperm.

MLH1 foci distribution

The distribution of foci on each autosomal SC has been analyzed (Figure 4a). MLH1 foci have been seen at all locations along the 22 autosomal SCs except at centromeres. This indicates that, at the resolution obtained using MLH1 immunocytogenetics (~10 Mb) (Lynn *et al*., 2004), almost any region of the genome is a possible target for crossing over. However, MLH1 foci are preferentially located at the subtelomere regions of all SCs, which seem to be the hottest recombination areas in the genome.

The two cases analyzed display similar distributions of hot and cold recombination regions in the SC set, despite the difference in the mean number of MLH1 foci per cell. Similar distributions have also been observed in three infertile cases (data not shown). However, particular differences have been detected between the C6 and the C7. A higher number of MLH1 foci in a specific SC arm (C7) makes the distal MLH1 focus be closer to the telomere while the proximal or medial parts become a little more prone to present an MLH1 focus. As an example, the SC8 in C6 generally shows two MLH1 foci (a mean of 1.90 MLH1 foci), whereas in C7 it can have two or three MLH1 foci (a mean of 2.35 MLH1 foci). Therefore, MLH1 distribution for SC8 in

Table III. Average number of MLH1 foci in each autosomal synaptonemal complex (SC) from the two cases

SC	*N*	MLH1 foci									Map units (cM) (mean)
		p arm			q arm			Bivalent			
		Mean	SD	Range	Mean	SD	Range	Mean	SD	Range	
1	212	1.76	0.56	0–4	1.58	0.54	0–3	3.34	0.83	1–6	167.2
2	213	1.34	0.55	0–3	1.90	0.52	0–3	3.23	0.76	1–5	161.7
3	213	1.41	0.54	0–3	1.40	0.55	0–3	2.81	0.77	1–5	140.6
4	212	0.98	0.26	0–2	1.60	0.63	0–3	2.58	0.69	1–4	129.2
5	212	0.94	0.26	0–2	1.71	0.58	0–3	2.65	0.63	1–4	132.3
6	213	1.11	0.36	0–2	1.35	0.54	0–3	2.46	0.66	1–4	123.2
7	213	1.07	0.36	0–2	1.40	0.51	0–2	2.47	0.66	1–4	123.5
8	213	0.93	0.27	0–2	1.19	0.51	0–2	2.13	0.58	0–3	106.3
9	213	0.95	0.22	0–1	1.26	0.48	0–3	2.21	0.53	1–4	110.3
10	213	0.96	0.19	0–1	1.31	0.57	0–2	2.28	0.59	1–3	113.8
11	212	0.99	0.17	0–2	1.19	0.49	0–3	2.18	0.53	1–4	109.2
12	213	0.90	0.31	0–2	1.44	0.56	0–3	2.34	0.61	1–4	116.9
13	213	0.01	0.12	0–1	1.78	0.50	0–3	1.79	0.51	0–3	89.7
14	213	0.01	0.10	0–1	1.67	0.55	0–3	1.68	0.56	0–3	83.8
15	213	0.02	0.14	0–1	1.82	0.49	1–3	1.84	0.52	1–3	92.0
16	213	0.97	0.20	0–2	0.95	0.23	0–2	1.92	0.30	1–3	96.0
17	212	0.90	0.30	0–1	1.02	0.34	0–2	1.92	0.42	1–3	96.2
18	213	0.66	0.48	0–1	1.02	0.30	0–2	1.68	0.54	0–3	84.0
19	213	0.89	0.31	0–1	0.97	0.26	0–2	1.86	0.42	0–3	93.0
20	213	0.76	0.43	0–1	0.88	0.36	0–2	1.63	0.50	0–3	81.7
21	213	0.01	0.12	0–1	0.95	0.21	0–1	0.97	0.25	0–2	48.4
22	213	0.01	0.10	0–1	1.14	0.41	0–1	1.15	0.42	0–2	57.5
Total	4,681							47.13			2352

Table IV. Percentage of synaptonemal complex (SC) with no MLH1

Case	SC							
	8	13	14	18	19	20	21	22
C6	0.95	0.95	0.95	1.9	3.81	0.95	4.76	3.81
C7	0.93		0.93				4.63	0.93

C7 resembles a tri-modal profile and in C6 a bimodal one (Figure 5a). However, the distribution of MLH1 foci in SC8s with the same number of foci is similar in both cases (Figure 5b). This is also true for other SCs. Therefore, despite the variability observed in the localization of MLH1 foci along the SC length, the MLH1 foci distribute in each SC following a similar pattern in different individuals.

MLH1 interfoci distances

The non-random localization of MLH1 foci in the SC set corroborates the existence of positive interference between foci observed in previous studies in humans (Barlow and Hultén, 1998; Lynn *et al*., 2002; Tease *et al*., 2002; Sun *et al*., 2004). MLH1 interfoci distance is expressed as the distance between two adjacent MLH1 foci in percentage of SC length. Mean interfoci distances for each SC with different numbers of MLH1 foci are shown (Figure 4b). Briefly (i) when two MLH1 foci are present in different arms within the SC (trans-centromere interfoci distance), these foci appear separated by a mean distance equivalent to about 70% of the SC length. In acrocentric SCs this is not a frequent situation, but when it occurs the trans-centromere interfoci distance is about 87%. (ii) When two MLH1 foci are located in the same arm (intra-arm interfoci distance), which is usually the q arm, the mean distance between foci is 38% (a range from about 25–50%). For acrocentric SCs this intra-arm interfoci distance increases to 57%. (iii) When three MLH1 foci are placed in an SC, the mean trans-centromere interfoci distance between two foci decreases to around 50% and the intra-arm interfoci distance to about 33% of the SC length. When it occurs in acrocentric SCs, the mean trans-centromere interfoci distance reduces to about 38% and the intra-arm interfoci distance to about 42% of the SC length. (iv) When four MLH1 foci are present in an SC (groups A, B and C, except SC8 and SC10), the trans-centromere interfoci distance is reduced to about 33% of the SC length and the intra-arm interfoci distance to about 25%. Thus, MLH1 interfoci distance has been observed to be dependent on the number of MLH1 foci and on their localization within the SC, as previously described (Sun *et al*., 2004). However, it is herein shown that acrocentric SCs display different interfoci distances compared to the non-acrocentric SCs.

The mean MLH1 interfoci distance comparison between SC1 and SC22 indicates that in terms of physical distance long chromosomes display more MLH1 interference than the short ones (10 μm and 3 μm, respectively), in agreement with previous observations in yeast (Kaback *et al*., 1999). However, our results demonstrate that when interfoci distance is expressed in terms of distance relative to the SC length, this relationship is inverted (37.3 and 59%, respectively). This effect is also observed when comparing between individuals with long (C7) and short (C6) SCs. For a given SC with the specific number of MLH1 foci, the C7 displays higher MLH1 interfoci distance in terms of physical length than the C6 but lower interfoci distance when considered as a percentage of the SC length. This could indicate that the intensity of interference between crossovers may be expressed as physical distance (μm) between foci and that it might modulate or be modulated by the total length of the SC. Whether SC length modulates or is modulated by interference remains still unclear; however, the proposal that chromosome axis length directly determines the crossover frequency (Kleckner *et al*., 2003) supports the idea that interference intensity might be modulated by the total SC length.

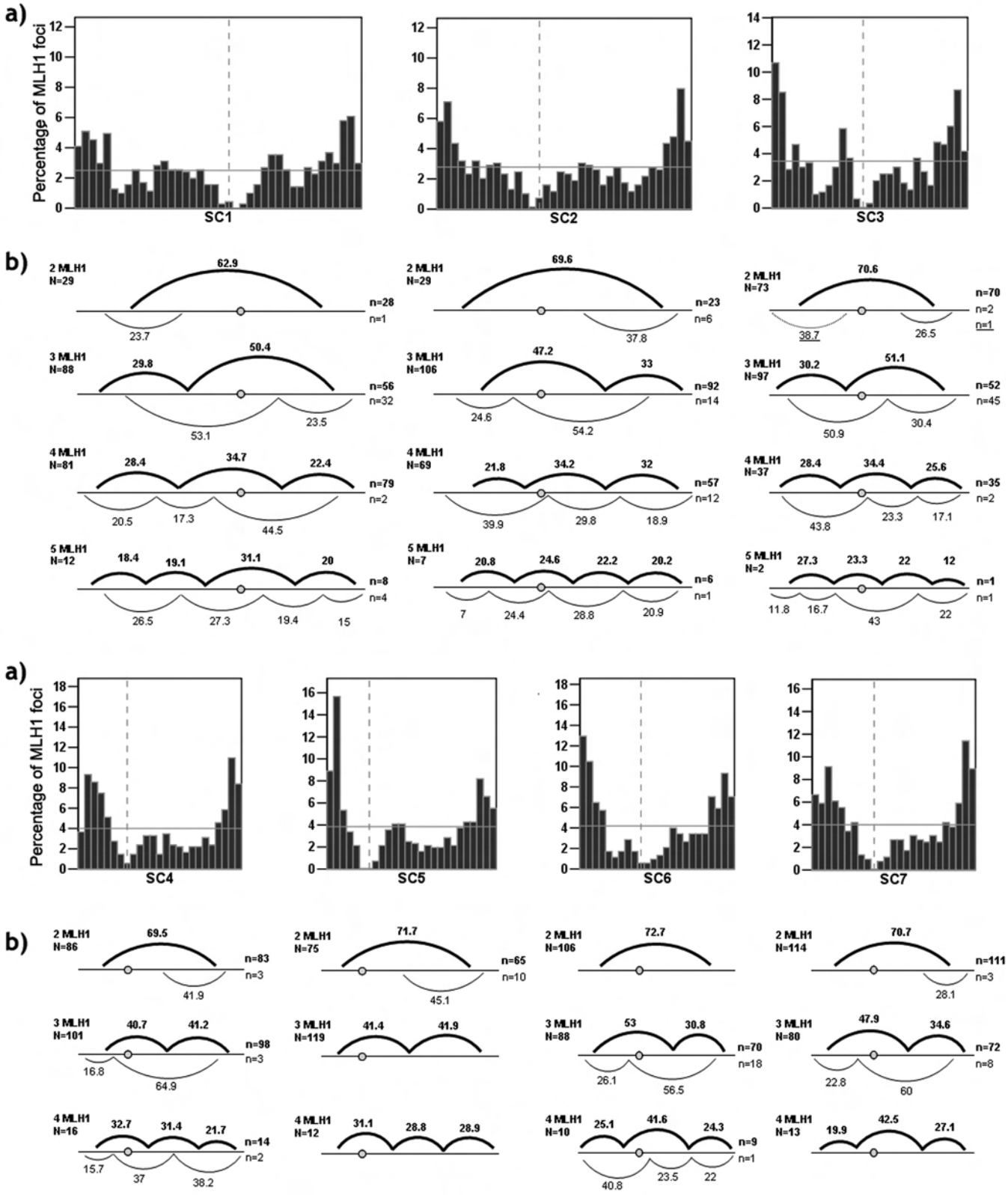

Figure 4. (**a**) General MLH1 distribution for individual synaptonemal complex (SC) is shown. Bars represent SC divisions of 0.7mm approximately. Bars indicate the probability of a single MLH1 focus to be placed in the region. The percentage of SCs that have an MLH1 focus in the region results from the product of each bar value and the mean of MLH1 foci in the SC (Table III). Centromere position is shown by the discontinuous vertical line. The horizontal line indicates the equal-probability line for which all MLH1 observed in a SC would be distributed at random. MLH1 distributions over this line indicate hot crossover regions while conversely, distributions under the line correspond to cold crossover regions. (**b**) Detailed distribution of the MLH1 foci in the SC and mean interfoci distances between adjacent foci are graphically presented for individual SCs. They are shown separately according to the number of MLH1 foci. Distances between MLH1 foci are expressed as a percentage of SC length. The bold line indicates the most frequent distribution of the MLH1 foci in the SC. The thin line indicates the least frequent distribution of the MLH1 foci in the SC.

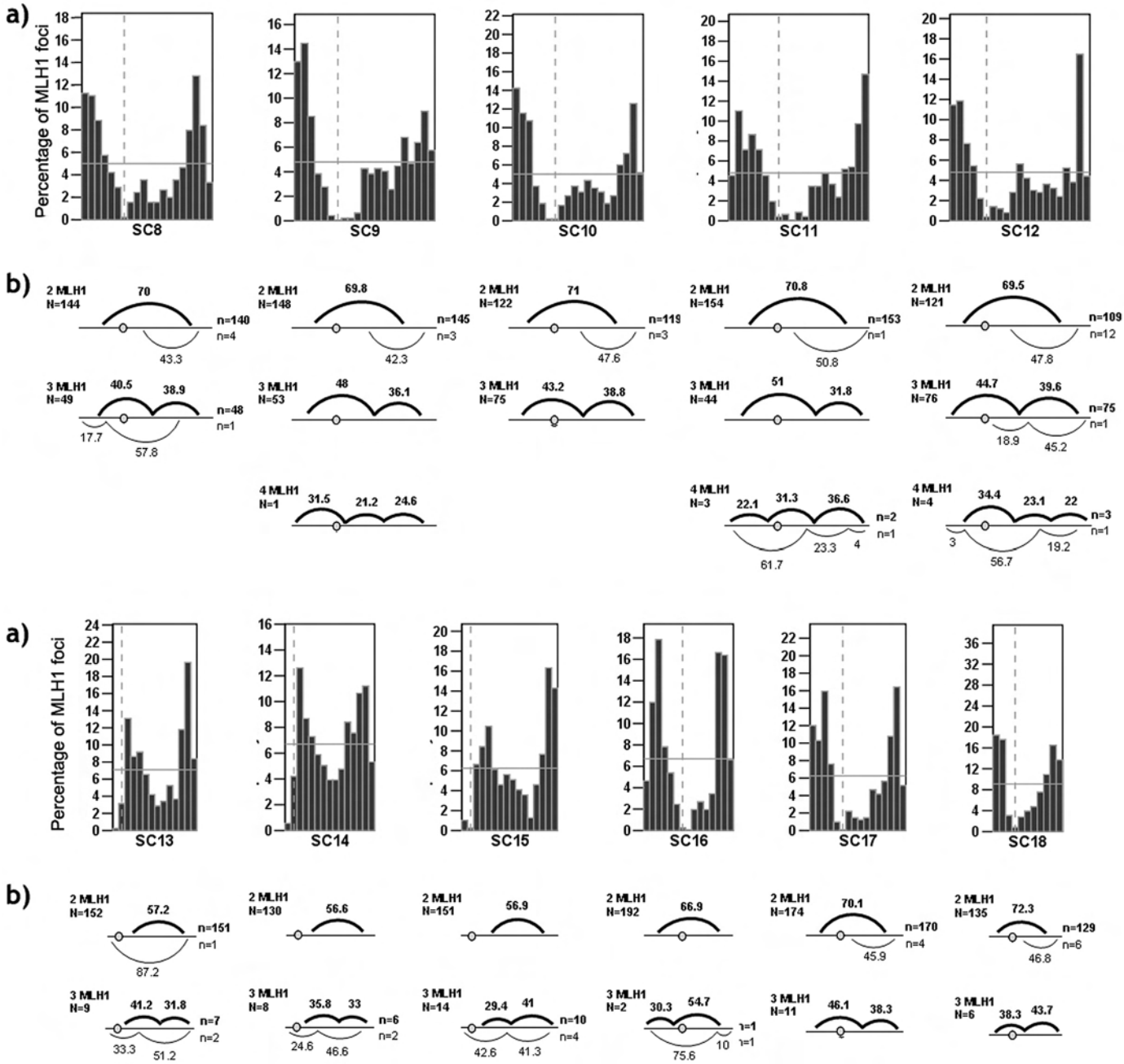

Figure 4. (*Continued*)

How may MLH1 foci distribute along the SC?

In the present study, the results from MLH1 distribution confirm that subtelomeric SC regions are hot regions for crossovers. As mentioned before, it is known that adjacent crossovers (i.e MLH1 foci) are evenly spaced and that they display positive interference (Barlow and Hultén, 1998; Lynn *et al*., 2002; Tease *et al*., 2002; Sun *et al*., 2004). A general idea for how interference works is that a crossover generates some crossover-discouraging signal or substance, which is spread for some distance along the chromosome. Several models have been proposed to explain how crossover interference acts. The counting model (Foss *et al*., 1993) proposes that each crossover is separated by a fixed number of non-crossover events, suggesting that cells may be able to 'count' recombination events. Recently, a new model based on mechanical forces has been proposed (Börner *et al*., 2004; Kleckner *et al*., 2004). This model suggests that meiotic chromosomes are under stress and that this stress is relieved at the crossover sites. Each crossover nucleation site spreads the stress release preventing the formation of a new crossover nearby (i.e. creating positive interference). A new crossover will occur only in places where the stress relief does not arrive and stress is accumulated.

In yeast, sites of crossing over have been reported to coincide with places of synaptonemal complex initiation (SIC) (Fung *et al*., 2004) suggesting that crossovers may directly promote the nucleation and spreading of the SC (Börner *et al*., 2004). Recently, it has been reported that in human males synapsis initiates at a limited number of subtelomeric SC sites and that it proceeds towards the centromere (Brown *et al*., 2005). All this data together with that presented in this study suggest that in humans the first crossovers to be designated in

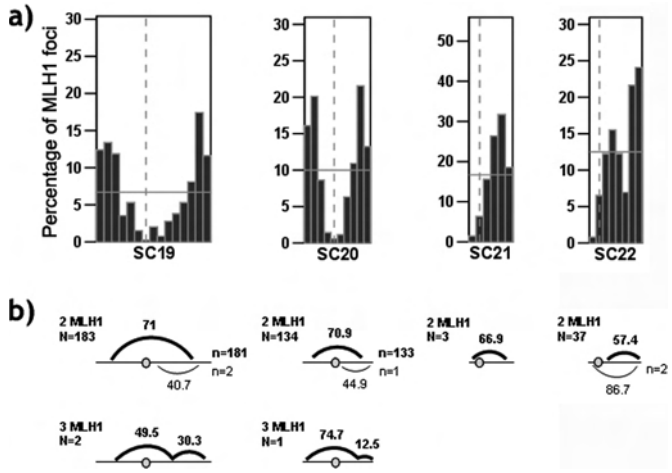

Figure 4. (*Continued*)

the crossover/non-crossover decision would be those in the subtelomeric regions where SC nucleation initiates. This, together with the existence of crossover interference, would explain why subtelomeric regions are hot regions for recombination. These first established crossovers would display interference. In direction towards the centromere, a new crossover would be positioned in the arm if it was long enough. This new crossover would consequently display interference, allowing the designation of an additional crossover in the same arm, but only if there was enough length. This might occur independently in both arms in metacentric and submetacentric SCs, as does the initiation of synapsis (Brown *et al*., 2005). If the arm length is not sufficient to place, another crossover interference would reach the centromere region. At the centromere, the interference coming from both sides of the SC would coincide, preventing the appearance of a new crossover in between. Therefore, trans-centromere interference would result from the sum of interference distances between the proximal crossovers in each arm and the centromere. Indeed, the interfoci distances in this study and in previous ones (Laurie and Hultén, 1985b; Sun *et al*., 2004) show that trans-centromere interference is higher than intra-arm interference.

However, the centromere itself may not directly interfere with crossing over, because sometimes MLH1 foci have been observed close to the centromere (e.g. large acrocentric SCs). It has been recently reported that the synapsis of acrocentric SCs starts at the q arms, but not at the p arms (Brown *et al*., 2005). According to this observation MLH1 foci interference in acrocentric SCs would only proceed from one side of the SC (i.e the q arm) towards the centromere. At the centromere region, interference would not coincide with any other one coming from the short arm and would allow the appearance of a new crossover close to the centromere in the q arm or in the p arm, if the distance of interference overpasses the centromere region (Figure 4a acrocentric SCs).

In summary, the stM-FISH assay allowed for the individual identification of all SCs and the unequivocal characterization of SC1p and SC1q arms. It is herein demonstrated that SC1p arms are longer than SC1q and that p and q arms may independently vary their relative length according to their GC and gene content. In addition, we suggest that the variation in the SC length might be an expression of the amount of open and compact chromatin fibers present in the region.

MLH1 interfoci distances are similar for all SCs with a specific number of MLH1 foci when expressed as a mean of percentage of their SC length. However, large SCs tend to show a higher mean MLH1 interfoci distance than the small ones only in terms of physical length, but not in distance relative to the SC. This indicates that interference would modulate its intensity according to the SC length.

Hot recombination regions are mainly located in distal parts of the SCs, with no differences between metacentric or submetacentric SCs. In acrocentric SCs subcentromere regions are also highly recombinant, indicating that, although MLH1 transcentromere interfoci distances are greater, the centromere does not create a direct negative effect on the localization of MLH1foci.

The main differences observed between the individual with a low crossover frequency and the one with a high one are shorter SCs, total absence of MLH1 focus in the p arm of acrocentric SCs, reduced frequency of XY pairs with an MLH1 focus, more SC19, SC22 and p arms of short SCs without MLH1 foci, and, finally, proximal-medial SC arm regions less prone to crossover.

The XY pair and SC21 are the bivalents that most frequently lack an MLH1 focus, consistent with the highest incidences of aneuploidy found in sperm nuclei for these chromosomes. Finally, reduction in

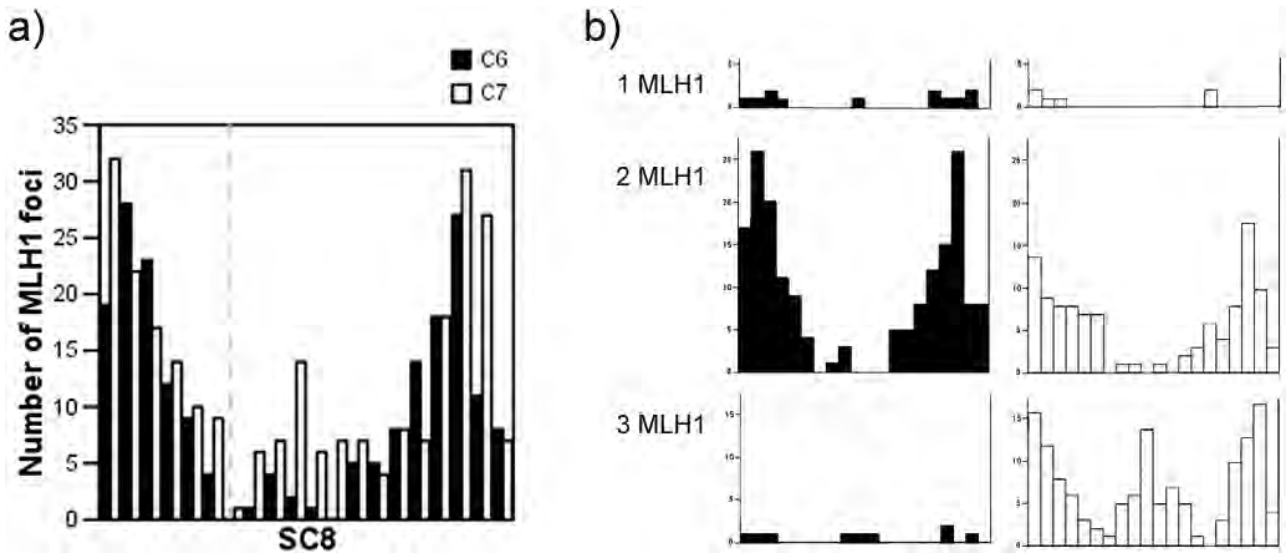

Figure 5. (**a**) Overall MLH1 distributions for SC8 in the two cases, displaying the lowest and the highest meiotic recombination frequency, respectively. (**b**) MLH1 distributions for SC8 presenting different numbers of recombination foci.

the general crossover frequency may increase the incidence of other achiasmate bivalents. Therefore, interindividual variation in the crossover frequency could explain the variability described for chromosome aneuploidies in human sperm.

Acknowledgements

We thank C. Abad, O. Arango, S. Egozcue, F. García and J. Sarquella for providing samples, Drs C. Heyting and W. Earnshaw for SCP1, SCP3 antibodies and CREST serum, respectively, and Dr C. Fauth for providing stM-FISH DNA pools. We also thank M. Oliver-Bonet for her critical reading of the manuscript. MCP was a recipient of a grant of the Generalitat de Catalunya (2001FI00468). This study was supported by the Fondo Investigación Sanitaria (Madrid) (Project PI051834), the Generalitat de Catalunya (Project 2005 SGR 00495) and the Deutsche Forschungsgemeinschaft (SP 460/4-1).

References

Baker SM, Plug AW, Prolla TA, Bronner CE, Harris AC, Yao X, Christie D-M, Monell C, Arnheim N, Bradley A et al (1996) Involvement of mouse Mlh1 in DNA mismatch repair and meiotic crossing over. Nat Genet 13,336–342.

Barlow AL and Hultén MA (1998) Crossing over analysis at pachytene in man. Eur J Hum Genet 6,350–358.

Baudat F, Manova K, Yuen JP, Jasin M and Keeney S (2000) Chromosome synapsis defects and sexually dimorphic meiotic progression in mice lacking Spo11. Mol Cell 6,989–998.

Börner GV, Kleckner N and Hunter N (2004) Crossover/noncrossover differentiation, synaptonemal complex formation, and regulatory surveillance at the leptotene/zygotene transition of meiosis. Cell 117,29–45.

Broman KW and Weber JL (2000) Characterization of human crossover interference. Am J Hum Genet 66,1911–1926.

Brown PW, Judis L, Chan ER, Schwartz S, Seftel A, Thomas A and Hassold TJ (2005) Meiotic synapsis proceeds from a limited number of subtelomeric sites in the human male. Am J Hum Genet 77,556–566.

Clyde JM, Hogg JE, Rutherford AJ and Picton HM (2003) Karyotyping of human metaphase II oocytes by multifluor fluorescence in situ hybridization. Fertil Steril 80,1003–1011.

Codina-Pascual M, Kraus J, Speicher M, Oliver-Bonet M, Murcia V, Sarquella J, Egozcue J, Navarro J and Benet J (2004) Characterization of all human male synaptonemal complexes by subtelomere multiplex-FISH. Cytogenet Genome Res 107,18–21.

Codina-Pascual M, Oliver-Bonet M, Navarro J, Campillo M, Garcia F, Egozcue S, Abad C, Egozcue J and Benet J (2005) Synapsis and meiotic recombination analyses: MLH1 focus in the XY pair as an indicator. Hum Reprod 20,2133–2139.

Egozcue S, Blanco J, Vendrell JM, García F, Veiga A, Aran B, Barri PN, Vidal F and Egozcue J (2000) Human male infertility: chromosome anomalies, meiotic disorders, abnormal spermatozoa and recurrent abortion. Hum Reprod Update 6,93–105.

Fauth C, Zhang H, Harabacz S, Brown J, Saracoglu K, Lederer G, Rittinger O, Rost I, Eils R, Kearney L et al. (2001) A new strategy for the detection of subtelomeric rearrangements. Hum Genet 109,576–583.

Foss E, Lande R, Stahl FW and Steinberg CM (1993) Chiasma interference as a function of genetic distance. Genetics 133,681–691.

Fung JC, Rockmill B, Odell M and Roeder GS (2004) Imposition of crossover interference through the nonrandom distribution of synapsis initiation complexes. Cell 116,795–802.

Gilbert N, Boyle S, Fiegler H, Woodfine K, Carter NP and Bickmore WA (2004) Chromatin architecture of the human genome: gene-rich domains are enriched open chromatin fibers. Cell 118,555–566.

Gutiérrez-Mateo C, Benet J, Wells D, Colls P, Bermudez MG, Sanchez-Garcia JF, Egozcue J, Navarro J and Munne S (2004) Aneuploidy study of human oocytes first polar body comparative genomic hybridization and metaphase II fluorescence in situ hybridization analysis. Hum Reprod 19,2859–2868.

Hassold T and Hunt PA (2001) To err (meiotically) is human: the genesis of human aneuploidy. Nat Rev Genet 2,280–290.

Hassold TJ, Sherman SL, Pettay D, Page DC and Jacobs PA (1991) XY chromosome nondisjunction in man is associated with diminished recombination in the pseudoautosomal region. Am J Hum Genet 49,253–260.

Hassold TJ, Judis L, Chan ER, Schwartz S, Seftel A and Lynn A (2004) Cytological studies of meiotic recombination in human males. Cytogenet Cell Genet 107,249–255.

Holmquist GP (1992) Chromosome bands, their chromatin flavors, and their functional features. Am J Hum Genet 51,17–37.

Hultén MA (1974) Chiasma distribution at diakinesis in the normal human male. Hereditas 76,55–78.

Hunter N and Kleckner N (2001) The single-end invasion: an asymmetric intermediate at the double-strand break to double-holliday junction transition of meiotic recombination. Cell 106,59–70.

ISCN (1985): An International System for Human Cytogenetic Nomenclature, Harnden DG and Klinger HP (eds); S.Karger, New York, 1985.

Kaback DB, Barber D, Mahon J, Lamb J and You J (1999) Chromosome size-dependent control of meiotic reciprocal recombination in saccharomyces cerevisiae: the role crossover interference. Genetics 152,1475–1486.

Kleckner N, Storlazzi A and Zickler D (2003) Coordinate variation in meiotic pachytene SC length and total crossover/chiasma frequency under conditions of constant DNA length. Trends Genet 19,623–628.

Kleckner N, Zickler D, Jones GH, Dekker J, Padmore R, Henle J and Hutchinson J (2004) A mechanical basis for chromosome function. Proc Natl Acad Sci USA 101,12592–12597.

Kong A, Gudbjartsson DF, Sainz J, Jonsdottir GM, Gudjonsson SA, Richardsson B, Sigurdardottir S, Barnard J, Hallbeck B, Masson G et al. (2002) A high-resolution recombination map of the human genome. Nat Genet 31,241–247.

Lammers JHM, Offenberg HH, van Aalderen M, Vink ACG, Dietrich AJJ and Heyting C (1994) The gene encoding a major component of the lateral elements of synaptonemal complexes of the rat is related to X-linked lymphocyte-regulated genes. Mol Cell Biol 14,1137–1146.

Laurie DA and Hultén MA (1985a) Further studies on bivalent chiasma frequency in human males with normal karyotypes. Ann Hum Genet 49,189–201.

Laurie DA and Hultén MA (1985b) Further studies on chiasma distribution and interference in the human male. Ann Hum Genet 49,203–214.

Lynn A, Koehler KE, Judis L, Chan ER, Cherry JP, Schwartz S, Seftel A, Hunt PA and Hassold TJ (2002) Covariation of synaptonemal complex length and mammalian meiotic exchange rates. Science 296,2222–2225.

Lynn A, Ashley T and Hassold T (2004) Variation in human meiotic recombination. Annu Rev Genomics Hum Genet 5,317–349.

Mahadevaiah SK, Turner JMA, Baudat F, Rogakou EP, de Boer P, Blanco-Rodríguez J, Jasin M, Keeney S, Bonner WM and Burgoyne PS (2001) Recombinational DNA double-strand breaks in mice precede synapsis. Nat Genet 27,271–276.

Matise TC, Sachidanandam R, Clark AG, Kruglyak L, Wijsman E, Kakol J, Buyske S, Chui B, Cohen P, de Toma C et al. (2003) A 3.9-centimorgan-resolution human single-nucleotide polymorphism linkage map and screening set. Am J Hum Genet 73,271–284.

Meuwissen RL, Offenberg HH, Dietrich AJ, Riesewijk A, van Iersel M and Heyting C (1992) A coiled-coil related protein specific for synapsed regions of meiotic prophase chromosomes. EMBO J 11,5091–5100.

Oliver-Bonet M, Liehr T, Nietzel A, Heller A, Starke H, Claussen U, Codina-Pascual M, Pujol A, Abad C, Egozcue J et al. (2003) Karyotyping of human synaptonemal complexes by cenM-FISH. Eur J Hum Genet 11,879–883.

Oliver-Bonet M, Turek PJ, Sun F, Ko E and Martin RH (2005) Temporal progression of recombination in human males. Mol Hum Reprod 11,517–522.

Revenkova E and Jessberger R (2005) Keeping sister chromatids together: cohesins in meiosis. Reproduction 130,783–790.

Roig I, Liebe B, Egozcue J, Cabero L, Garcia M and Scherthan H (2004) Female-specific features of recombinational double-stranded DNA repair in relation to synapsis and telomere dynamics in human oocytes. Chromosoma 113,22–33.

Romanienko PJ and Camerini-Otero RD (2000) The mouse Spo11 gene is required for meiotic chromosome synapsis. Mol Cell 6,975–987.

Sarrate Z, Blanco J, Egozcue S, Vidal F and Egozcue J (2004) Identification of meiotic anomalies with multiplex fluorescence in situ hybridization: preliminary results. Fertil Steril 82,712–717.

Savage A, Petersen M, Pettay D, Taft L, Allran K, Freeman S, Karadima G, Avramopoulos D, Torfs C, Mikkelsen M et al. (1998) Elucidating the mechanisms of paternal non-disjunction of chromosome 21 in humans. Hum Mol Genet 7,1221–1227.

Shi Q, Spriggs E, Field L, Ko E, Barclay L and Martin RH (2001) Single sperm typing demonstrates that reduced recombination is associated with the production of aneuploid 24,XY human sperm. Am J Med Genet 99,34–38.

Stack SM (1984) Heterochromatin, the synaptonemal complex and crossing over. J Cell Sci 71,159–176.

Sun F, Oliver-Bonet M, Liehr T, Starke H, Ko E, Rademaker AW, Navarro J, Benet J and Martin RH (2004) Human male recombination maps for individual chromosomes. Am J Hum Genet 74,521–531.

Sun F, Trpkov K, Rademaker AW, Ko E and Martin RH (2005) Variation in meiotic recombination frequencies among human males. Hum Genet 116,172–178.

Svetlanov A and Cohen PE (2004) Mismatch repair proteins, meiosis, and mice: understanding the complexities of mammalian meiosis. Exp Cell Res 296,71–79.

Tease C, Hartshorne GM and Hultén MA (2002) Patterns of meiotic recombination in human fetal oocytes. Am J Hum Genet 70,1469–1479.

Templado C, Bosch M and Benet J (2005) Frequency and distribution of chromosome abnormalities in human spermatozoa. Cytogenet Genome Res 111,199–205.

Thomas NS, Collins AR, Hassold TJ and Jacobs PA (2000) A reinvestigation of non-disjuntion resulting in 47,XXY males of paternal origin. Eur J Hum Genet 8,805–808.

Venter CJ, Adams MD, Myers EW, Li PW, Mural RJ, Sutton GG, Smith HO, Yandell M, Evans CA et al. (2001) The sequence of the human genome. Science 291,1304–1351.

Yokota H, Singer MJ, van den Engh GJ and Trask BJ (1997) Regional differences in the compaction of chromatin in human G0/G1 interphase nuclei. Chromosome Res 5,157–166.

Submitted on November 18, 2005; accepted on December 28, 2005